Influence of nonstationarity on reservoir storage-yield-reliability relationships

Influência da não estacionariedade nas curvas de regularização de reservatórios de usinas hidrelétricas

Henrique Degraf[1] ![ORCID] **& Daniel Henrique Marco Detzel**[1] ![ORCID]

[1]Universidade Federal do Paraná, Curitiba, PR, Brasil
E-mails: degraf.henrique@gmail.com (HD), detzel@ufpr.br (DHMD)

ABSTRACT

The reservoir storage-yield-reliability (S-Y-R) curve defines the required volume to meet a specific yield. It is typically obtained through the historical streamflow time series; however, as an effect of nonstationarity, the statistical properties of a streamflow series may vary, which might lead to a change in the reservoir's operational risk. In this study we explore this issue by analyzing two sets of annual data: (i) natural energy flows to aggregated reservoirs, and (ii) streamflow time series of four hydropower plants currently in operation in Brazil. The study is supported by Monte Carlo simulations to account for the reliability of the S-Y-R curves. Results suggest that the time series from the Southern and Northeast regions exhibit upward and downward trends, respectively. Consequently, the regularization capacity of the Southern reservoir decreased, however only in relative terms. On the other hand, the Northeastern reservoir had an actual loss of its regularization capacity as an effect of lower average streamflow.

Keywords: Trend; Storage-yield-reliability curve; Reservoir; Regularization.

RESUMO

A curva de regularização é obtida a partir das séries históricas de vazão e determina as demandas possíveis de serem atendidas para diferentes volumes dos reservatórios. Contudo, como efeito da não estacionariedade as estatísticas relacionadas às séries históricas podem variar com o tempo, o que reflete em uma alteração no risco de operação dos reservatórios. Este estudo explora a questão analisando dois conjuntos de dados: (i) energias naturais afluentes a reservatórios equivalentes e (ii) séries de vazões afluentes a quatro usinas hidrelétricas em operação. Simulações de Monte Carlo são utilizadas para a obtenção de faixas de confiabilidade das curvas. Os resultados mostram que as séries temporais das regiões Sul e Nordeste do Brasil apresentaram tendências de aumento e redução, respectivamente. Consequentemente, a capacidade de regularização do reservatório ao Sul decaiu, mas somente em termos relativos. Por outro lado, o reservatório no Nordeste apresentou uma perda na capacidade de regularização por efeito do decaimento na vazão média.

Palavras-chave: Tendências; Curva de regularização; Reservatório; Regularização.

INTRODUCTION

Reservoirs are a necessary intervention of humanity in nature. Water supply, water storage, energy generation, flood containment, and agriculture irrigation, are some of their main uses (Carvalho, 2015). The water storage capacity is fundamental for the development of societies and countries, promoting the meeting of the population's water and energy needs (Briscoe, 2011). In Brazil, water resource represents about 60% of the country's electric matrix (Agência Nacional de Energia Elétrica, 2022), which is essential for maintaining the matrix predominantly renewable. Such a percentage is comprised of about 165 large hydropower plants (HPPs) (with more than 30 MW of installed capacity) currently in operation; among them, 72 have reservoirs with an over-year storage capacity (Operador Nacional do Sistema Elétrico, 2020).

A common method to associate water supply yields with a certain reservoir's active volume is the storage-yield-reliability curve (S-Y-R). It consists of a nonlinear function that relates a constant release rate with the required storage for a given reliability (Loucks & van Beek, 2005, p. 344). The S-Y-R relationship was thoroughly studied by R. Vogel and collaborators circa 1980-90 in a series of papers that explored its statistical properties (Vogel & McMahon, 1996; Vogel & Bolognese, 1995; Vogel & Stedinger, 1987, 1988) and applications in the United States (Vogel et al., 1995, 1997, 1999). More recently, the S-Y-R curve has been widely used not only for designing purposes (Silva & Portela, 2013; McMahon et al., 2007) but also as a tool for understanding the operating rules of existing reservoirs (Aljoda & Jain, 2021; Srivastava & Awchi, 2009; Vogel et al., 2007). Moreover, Kuria & Vogel (2015) employed the S-Y-R relationship to evaluate the uncertainty of water supply reservoir yields.

The streamflow time series is the main input to define the S-Y-R curve, thereby any changes in this series can produce variations in the curve as well. In this sense, anthropogenic climate change (Milly et al., 2015), land-use modifications (Mo et al., 2020; Levy et al., 2018), or a combination of both (Guo et al., 2020), are frequently highlighted as inductors of nonstationarities in streamflow time series. Climate change is referred to an increase in temperature triggered by the growth of greenhouse gas emissions (Gleick, 1989). The consequence is a modification in the precipitation patterns, with an increase in the occurrence of extreme events (wet and dry) in diverse regions of the globe (Dore, 2005). In turn, land-use transformations alter the terrestrial-related phases of the hydrological cycle (Brown et al., 2005). Nonetheless, separating these causes is a challenging task in hydrological research; for example, Wang et al. (2013) list several studies that attempt to do so by using diverse approaches that include statistical, climate-based, and hydrological models. The authors themselves obtained consistent results by applying three different approaches to a study case in China. However, they emphasized that errors and uncertainties are non-neglectable in the processes.

Even with an incomplete understanding of the causes that lead river regimes to change, trends in streamflow time series have been detected worldwide (Gudmundsson et al., 2019) and in diverse regions in Brazil. For example, Chagas & Chaffe (2018) identified a general increase in annual mean flow in the southern region of the country, with statistically significant trends in Iguazu and Uruguay river basins. Overall, these changes followed an increase also observed in the mean annual rainfall in the region. However, the authors show that the increase rate of the streamflow is higher than the rainfall, suggesting that land-use modifications may also be relevant. Silva et al. (2019) obtained similar results for the Paraná River basin at the Itaipu HPP location. On the other hand, the authors detected decreasing trends in the São Francisco River streamflow at the Sobradinho and Xingó HPPs locations. Interestingly, such changes were not detected for the rainfall time series. In turn, de Jong et al. (2018) pointed out that the São Francisco River has consistently been showing decreasing streamflows since the early 90s because of the combination of rainfall reduction and water withdrawals for irrigation purposes.

Freitas (2020) also detected negative trends in inflows to two of the four reservoirs of the Cantareira system, in the Metropolitan Region of São Paulo. This is an important water supply system that suffered from extreme drought in 2013-2015, with severe socioeconomic consequences. Even so, no trends were detected in precipitation; hence, land-use changes were pointed as the main cause for streamflow reduction. In northern Brazil, Heerspink et al. (2020) detected both increasing and decreasing trends in streamflows of the Amazon River basin. The explanation relied on an interaction between climatic and land-use changes, with a contribution of groundwater storage variation due to deforestation.

As seen by the cited references, several studies have been conducted on streamflow nonstationarity, aiming at pointing at possible explanations. Nevertheless, only a few addressed its impacts on the reservoir's operation and reliability. For instance, Ehsani et al. (2017) showed that the variation in the statistical parameters can increase the reservoirs' operational risk. The authors advocate that the importance of dams will increase in a climate change scenario. Moreover, in studying the Oroville Dam (California, United States), Aljoda & Jain (2021) argued that the reservoir performance is affected significantly by streamflow nonstationarity. Both studies were conducted locally, and it is our understanding that the link between S-Y-R relationships and trends in the streamflow time series needs further investigation. This is particularly important in Brazil, for its strong dependence on hydropower plants.

Hence, this paper investigates the possible impacts of the nonstationarity on the hydropower plants reservoir's S-Y-R curves, analyzing the regularization capacity variability over the years. First, we consider a territorial-wide analysis, using the energy equivalent reservoirs (EER) approach (Larroyd et al., 2017). It is a solution commonly adopted in Brazil that aggregates all hydropower plants in four EERs (Southeast/Central-West, South, Northeast, and North subsystems). In this sense, the streamflows are converted to natural energy flows (*ENAs*, average MW – MWa) and reservoirs are represented in average energy units (MW-month). Then, we deepen the analysis to four relevant reservoirs that operate in all subsystems, namely: Foz do Areia (South, Iguazu River), Ilha Solteira (Southeast/Central-West, Paraná River), Sobradinho (Northeast, São Francisco River), and Tucuruí (North, Tocantins River). In this latter analysis, we consider the originally designed S-Y-R relationship and compare it with an updated S-Y-R relationship. In both cases,

trends and breakpoints in *ENAs* and streamflows are assessed by Mann-Kendall and Pettitt tests (Fleming & Weber, 2012).

METHODS

To perform the analyses, we followed the steps of the workflow depicted in Figure 1. They are similar for both EER and individual reservoir cases, with an additional step for the EER case regarding the determination of the *ENAs* time series. First, the nonstationarity of each time series is assessed by v applying statistical inferences. If necessary, a correction procedure is applied to the series in order to feed stationary inputs into a stochastic model based on an autoregressive [AR(p)] formulation. It is worth noting that we must submit stationary series to the stochastic model because it follows a formulation that is stationary by definition. Although nonstationary stochastic linear models are available (e.g. ARIMA models, see Box et al., 2008), they are not suitable for synthetic series generation, since the variance of the nonstationary process tends to infinity (Salas et al., 1985, p. 281). Once the synthetic series are generated, the S-Y-R curves are obtained and analyzed.

On an important note, we do not intend to explain the causes of the detected nonstationarities. Rather, we focus on the possible effects of these phenomena on the S-Y-R relationships. Hence, any investigation involving climate or land-use changes in the studied catchments is out of the scope of this paper. For the reader interested in such topics, we recommend the references cited in the introductory section.

The following sections provide the equations and methodological details for each step.

Considered dataset

For this paper, we obtained all the datasets from the SINtegre web portal (https://sintegre.ons.org.br), which is maintained by the Electric System National Operator (ONS). The data includes all 165 HPPs' information and the streamflow data, the latter ranging from 1931 to 2020, on an annual time scale. The annual scale was used to agree with the over-year regularization capacity of the considered reservoirs. Also, it is the common scale adopted in S-Y-R analyses (Vogel & McMahon, 1996; Vogel & Bolognese, 1995; Vogel & Stedinger, 1987, 1988).

Streamflow time series are associated with the damming locations. It is worth mentioning that ONS provides naturalized streamflow data, in which the dam effects on the rivers, HPPs operation, water withdrawals, and lake evaporation losses are disregarded (see Braga et al., 2009). Also, in rivers with several reservoirs (e.g. cascade of reservoirs), the cumulative effects of the HPPs are taken into account as well.

As mentioned earlier, we first analyzed the *ENAs* time series for the four main EER reservoirs that constitute the Brazilian National Interconnected System (SIN). The ONS also provides *ENAs* time series for the same periods of the streamflow time series, however, it does not describe which HHPs are considered in the process. To avoid consistency problems regarding the HPPs set used in our and ONS studies, we chose to recalculate the *ENAs* time series for each EER.

The *ENA* time series (MWa) for the subsystem *s* is obtained by applying Equation 1 (Neira, 2005):

$$ENA_{s,t} = \sum_{u=1}^{U_s} \frac{\left(9,81 \cdot h_u \cdot \eta_u\right)}{1000} \cdot Q_{u,t} \tag{1}$$

where U_s is the total number of HPPs of the subsystem *s*, and h_u (m) and η_u (dimensionless) are the net head and turbine-generator efficiency of the HPP *u*, respectively. $Q_{u,t}$ (m³/s) is the (natural) affluent streamflow of the HPP *u* at time *t*.

We also investigated the S-Y-R relationships of four SIN HPPs, located in different parts of the Brazilian territory (Figure 2 and Table 1). To choose the HPPs, we elected plants with large generation and useful storage capacities in each of SIN's subsystems.
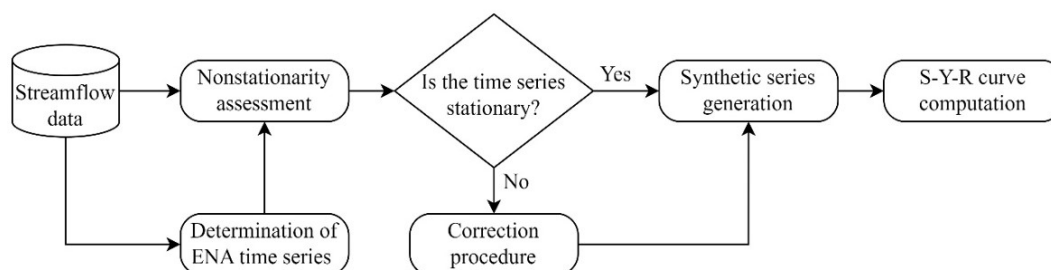

Figure 1. Workflow of the proposed methodology. The procedure is applied individually for each considered time series.

Table 1. HPPs main information.

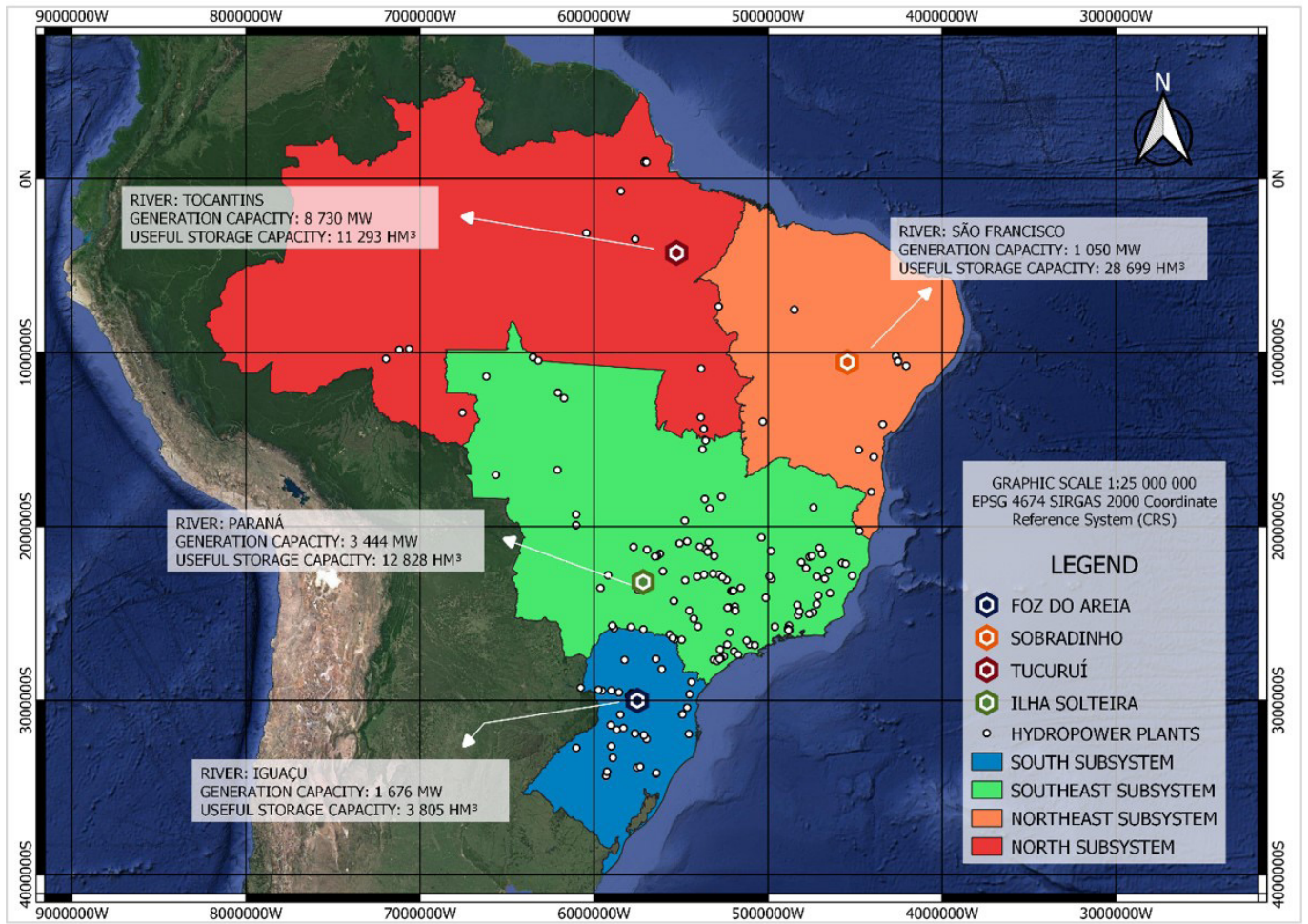| HPP	Basin	Opening date	Operator	Generation capacity (MW)	Useful storage capacity (hm³)
Ilha Solteira	Paraná	1973	CESP	3444	12828
Foz do Areia	Iguazu	1981	COPEL	1676	3805
Sobradinho	São Francisco	1979	CHESF	1050	28669
Tucuruí	Tocantins	1984	ELETRONORTE	8730	11293

Figure 2. SIN's subsystems and HPPs location. The four studied HPPs are highlighted.

Besides, they are submitted to distinct hydrologic regimes. Table 1 also provides the opening date of each HPP, which we use as a reference for our analysis.

Nonstationarity assessment

The *ENA* and streamflow time series were submitted to Mann-Kendall (Mann, 1945; Kendall, 1975) and Pettitt (1979) tests to check for nonstationarity. The Mann-Kendall test considers all elements of a series z_t as equiprobable. If the null hypothesis is rejected, the existence of a trend cannot be disregarded. The test statistic *MK* is obtained from Equation 2:

$$MK = \sum_{i=1}^{n-1} \sum_{j=i+1}^{n} \text{sgn}\left[z_j - z_i\right] \tag{2}$$

where,

$$\text{sgn}\left[z_j - z_i\right] = \begin{cases} 1, & \text{if } \left(z_j - z_i\right) > 0 \\ 0, & \text{if } \left(z_j - z_i\right) = 0 \\ -1, & \text{if } \left(z_j - z_i\right) < 0 \end{cases} \tag{3}$$

Next, a standard normal variable is obtained by applying:

$$z = \begin{cases} \dfrac{MK - 1}{\sqrt{VAR\left[MK\right]}}, & \text{if } MK > 0 \\ 0, & \text{if } MK = 0 \\ \dfrac{MK + 1}{\sqrt{VAR\left[MK\right]}}, & \text{if } MK < 0 \end{cases} \tag{4}$$

where,

$$VAR\left[MK\right] = \frac{n\left(n-1\right)\left(2n+5\right)}{18} \tag{5}$$

The null hypothesis is rejected if $z \geq z_{\alpha/2}$ for a given significance level α.

In turn, the Pettitt test checks for breakpoints in the series, which is also an indicator of nonstationarity. The test statistic is computed from Equation 6:

$$PT\left(\tau\right) = \sum_{i=1}^{\tau} \sum_{j=\tau+1}^{n} \text{sgn}\left[z_j - z_i\right] \tag{6}$$

where τ represents the change point in a series z_t. Note that $\text{sgn}[\,]$ is obtained by the same Equation 3 previously shown. The test significance α_0 is determined by the approximation shown in Equation 7:

$$\alpha_0 \sim 2 \cdot \exp\left(\frac{-6PT^2}{n^3 + n^2}\right) \qquad (7)$$

where,

$$PT = MAX\left|PT(\tau)\right|, \quad 1 \le \tau \le n \qquad (8)$$

The null hypothesis is rejected if $\alpha_0 < \alpha$, for a given significance level α. In this paper, we considered $\alpha = 0.05$ for both Mann-Kendall and Pettitt tests.

It is worth noting that we checked all series for significant autocorrelation before applying the tests. It is well-known that the persistence of a series, if relevant, may indicate nonexistent nonstationarities (i.e., type I error) (Fleming & Weber, 2012). In such situations, we applied a prewhitening procedure (Yue et al., 2002) to remove the dependence structure of the series.

Finally, in cases where nonstationarity cannot be rejected (i.e., rejection in any Mann-Kendall or Pettitt tests), we performed a correction procedure based on Detzel et al. (2011). In this approach, streamflow (or *ENA*) time series are accumulated over time and the angular coefficients are obtained for the periods before (c_1) and after (c_2) the breakpoint indicated by the Pettitt test. Next, the accumulated series from the first period is multiplied by the ratio between the angular coefficients (c_1 / c_2).

S-Y-R relationship computation

The first step to obtaining the S-Y-R relationship for a reservoir is the determination of its regularization curve. Mathematically, the regularization curve can be represented by a function $Z = f(V)$, where a different storage level V leads to a certain firm yield Z. For the purpose of this paper, both storage and yield can be expressed either in volume or energy units (m^3 and m^3/s or MWa, respectively). In any case, the yields are established as a function of the regularization index δ, defined by Equation 9:

$$\delta = \frac{Z}{\bar{Z}}, 0 \le \delta \le 1 \qquad (9)$$

where $\bar{Z}$ is the mean of Z. Physically, Equation 9 expresses that the maximum regularization capacity of any reservoir is the long-term mean of its inflows. To compute the different storage levels V (and respective yields Z), we applied the sequent peak analysis method (Loucks & van Beek, 2005, p. 343), which is based on the maximum cumulative deficit D:

$$V = \max D_t \qquad (10)$$

where,

$$D_t = \max \begin{cases} 0 \\ D_{t-1} - Z_t + \delta\bar{Z} \end{cases} \qquad (11)$$

In Equation 11, Z can assume either streamflow or *ENAs* time series.

To measure the reservoir's reliability through the regularization curves, we used a Monte Carlo approach based on synthetic series generation with an autoregressive model [AR(p)] applied to all the series. The fitting process was performed following the Box-Jenkins iterative identification-estimation-validation method for stochastic linear model building (Box et al., 2008). First, as

a requirement for applying Box-Jenkins formulation, all series were tested for normality. For the series that were not normal, logarithmic transformation was applied (Table 2).

Next, autocorrelation (FAC) and partial autocorrelation (FACP) functions were plotted to identify the order of the models. Figure 3 depicts such functions for the ENAs time series. From a visual analysis, the FAC and FACP of the Southeast/Central-west subsystem (Figure 3a) suggest a first-order autoregressive model [AR(1)] (exponential decay of the FAC and the significant first lag of the FACP). For the Northeast subsystem (Figure 3b), the similar behavior of the FAC and FACP functions suggests that a moving average term should be included in the model; however, its order is unclear. Moreover, the analysis of functions of the remainder subsystems was inconclusive, since all the autocorrelations and partial autocorrelations lay inside the 0.05 significance band. The results for the HPP's streamflows were similar and not shown.

To support the decision regarding the model to be adopted, their goodness-of-fit was further investigated with information criteria metrics, such as the Akaike (AIC) and Bayesian Information Criteria (BIC) (Akaike, 1974; Schwartz, 1978). Since first-order models are common in modeling annual streamflow for reservoir storage-related studies (Vogel & McMahon, 1996), AIC and BIC were calculated for AR(1) and ARMA(1,1) models. As a result, AR(1) model was pointed as the best formulation in all cases (Table 3).

Table 2. P-values of the normality test applied to the SIN EERs and studied HPPs. Bold p-values indicate null hypothesis rejection at a 0.05 significance level. For the non-normal series, logarithmic transformation was applied and submitted to the same test for normality confirmation.

ENA/HPP	Original Series	Log-transformed series
Southeast/Central-west	0.13	-
South	**< 0.01**	0.06
Northeast	**< 0.01**	0.76
North	0.57	-
Foz do Areia	**0.02**	0.14
Ilha Solteira	**< 0.01**	0.08
Sobradinho	**0.02**	0.79
Tucuruí	**0.02**	0.98

Table 3. AIC and BIC for AR(1) and ARMA(1,1) models fitted to ENAs and HPPs time series. The best model is the one that results in the minimum value of each criterion (in bold).

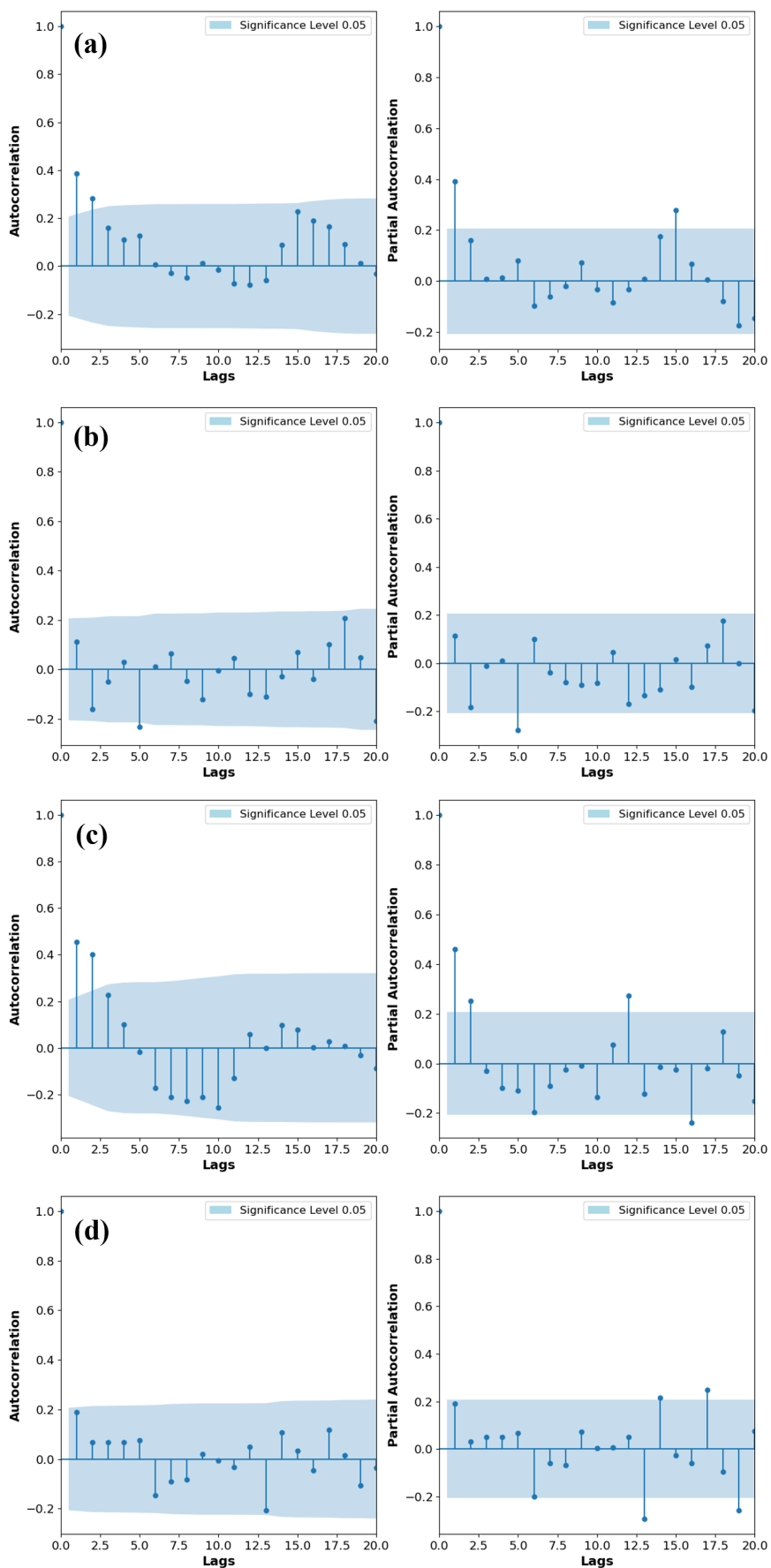| ENA/HPP	AR(1)		ARMA(1,1)	
	AIC	BIC	AIC	BIC
Southeast/Central-west	**-245.80**	**-245.43**	-246.32	-243.60
South	**1554.32**	**1554.68**	1556.43	1559.15
Northeast	**-154.74**	**-154.37**	-160.85	-158.13
North	**1488.66**	**1489.02**	1490.71	1493.43
Foz do Areia	**590.54**	**590.22**	592.81	594.16
Ilha Solteira	**641.97**	**641.43**	644.16	645.07
Sobradinho	**-85.84**	**-86.21**	-83.91	-82.66
Tucuruí	**-96.12**	**-96.37**	-95.11	-93.62

Figure 3. Autocorrelation (left panel) and partial autocorrelation (right panel) functions for the ENAs of SIN's subsystems (a) Southeast/Central-west, (b) South, (c) Northeast, and (d) North.

Once the models were fit to the series, the residuals were tested for normality, homoscedasticity, and independence, following the procedures suggested by Salas et al. (1985). The results in Table 4 show no rejections of any of the assumptions for a 0.05 significance level. Hence, the AR(1) model was confirmed as an appropriate method for the synthetic series generation.

Finally, to obtain the S-Y-R we followed the step-by-step iterative framework depicted below:

1. Generate N synthetic series with size n'

2. Adopt a return period T_r

3. Adopt a regularization index δ

4. Calculate the storage levels for the N generated series. The results may be organized in a vector V_N

5. Sort the resulting V_N vector in ascendent order

6. Calculate the probability of success p associated with T_r by applying:

$$p = \left(1 - \frac{1}{T_r}\right)^m \qquad (12)$$

where m is the reservoir lifespan. Here, the probability of success is referred to as the success of the reservoir to meet its demand. Also, p expresses the reservoir reliability.

7. Search in the sorted V_N vector the element of order $(n' \cdot p)$. This element is the storage level associated with the regularization index δ for the adopted T_r

8. Change δ and return to step 3

9. Change T_r and return to step 2.

For this work we adopted $N = 1000$, δ varying in 10% intervals, $m = 50$ years, and a set of $T_r = \{10, 25, 50, 100, 200, 250, 500\}$ years. As with n', for the *ENAs* we generated synthetic series of the same size as the historical dataset (90 years). For the streamflows, we generated two independent sets of scenarios: (i) with the AR(1) model estimated considering the historical time series ranging from 1931 until the opening date of each HPP (see Table 1); (ii) with the AR(1) model estimated with the entire dataset. With this approach, we intend to compare the S-Y-R relationships in two distinct moments in each reservoir's history.

RESULTS AND DISCUSSIONS

Nonstationarity

Table 5 shows the results of the nonstationarity tests applied to the four EERs. The South and Northeast subsystems presented significant trends, as indicated by the Mann-Kendall test p-values. A further investigation of these trends revealed that the trend direction is opposite for the EERs: while the South *ENA* presented an increasing trend, the Northeast *ENA* is decreasing over time. In the first case, this behavior is well-known and was indicated in earlier studies such as Detzel et al. (2011). More recently, Lee et al. (2018) argued that such changes are a consequence of land-use transformations that have been taking place in the Paraná River basin over the last 40 years. Conversely, Abou Rafee et al. (2022) suggest that the climate shift that occurred between 1974 and 1977, played a major role in the changes observed in the mean annual streamflow of the Upper Paraná River Basin. It is worth noting that the Pettitt test indicated a significant breakpoint exactly in 1970.

On the other hand, the decreasing trend of the Northeast ENA was only statistically detected recently (Silva et al., 2019). The region suffered a severe drought episode in the 2010s (Jong et al., 2018), which may justify such results. However, the Pettitt test indicated a breakpoint roughly 20 years earlier. We argue that this result should be explored in further studies, as it suggests that changes in Northeast ENA might have been taking place longer than the studies have shown.

Finally, the Southeast/Central-West and North did not show any nonstationarities. Nonetheless, this result does not discard the possibility of nonstationarities of individual streamflow time series, as the aggregation procedure for obtaining the time series might cover up such occurrences.

In turn, Table 6 shows the results of the nonstationarity tests applied to the four HPPs. The results for the individual HPPs

Table 4. P-values for normality, homoscedasticity, and independence tests applied to the residuals obtained from the fitted AR(1) for all series. No rejections were found for a 0.05 significance level.

ENA/HPP (residuals)	Normality	Homoscedasticity	Independence
Southeast/ Central-west	0.67	0.21	0.76
South	0.09	0.81	0.53
Northeast	0.86	0.29	0.23
North	0.09	0.37	0.56
Foz do Areia	0.48	0.43	0.20
Ilha Solteira	0.63	0.14	0.54
Sobradinho	0.10	0.82	0.78
Tucuruí	0.49	0.26	0.70

Table 5. P-values of the nonstationarity tests applied to the SIN EERs. Bold p-values indicate null hypothesis rejection at a 0.05 significance level. The signs in Mann-Kendall test results suggest increasing (+) or decreasing (–) trends.

EER	Prewhitening	Mann-Kendall		Pettitt	
		p-value	Trend sign	p-value	Breakpoint (year)
Southeast/Central-west	Yes	0.33	+	0.09	1970
South	**Yes**	**0.01**	+	**0.03**	1970
Northeast	**Yes**	**0.03**	–	**0.02**	1991
North	No	0.29	–	0.55	1997

are similar to the results for the EERs in which they operate, with subtle differences in the p-values. Foz do Areia shows a significant positive trend, however no significant breakpoint. In Sobradinho both p-values for the Mann-Kendall and Pettitt tests indicate nonstationarity. The latter suggested 1992 as the year of the breakpoint. Lastly, the overall stationarity condition of Ilha Solteira and Tucuruí time series was maintained.

In EERs or HPPs with significant trends is natural to expect changes in the S-Y-R relationships, as the regularization index explicitly considers the long-term mean on its equation [see Equation 9]. Hence, increasing trends in series may lead to a decrease in the regularization capacity and vice-versa. This question is investigated in the S-Y-R relationships results section.

Synthetic series validation

Prior to the determination of the S-Y-R relationships, the generated synthetic series were validated by exploratory data analysis. The employed metrics were mean (M), standard deviation (SD), coefficient of variation (CV), skewness (SK), minimum streamflow (min), maximum streamflow (max), and first-order autocorrelation (AC1). In addition, two drought-related statistics were calculated: longest drought period (LD) and maximum deficit (MD). All the

metrics were computed for both historical and generated series, for comparison purposes. Yet, for the nonstationary series, the statistics of the original and corrected time series are both shown. Table 7 and Table 8 exhibits the results for $ENAs$ and streamflow time series, respectively.

For all the series, the AR(1) model performed well in reproducing the metrics. Minor inaccuracies were detected in the skewness of the synthetic scenarios obtained for the South and North $ENAs$, and for Foz do Areia HPP. For the nonstationary time series, it is important to recall that the stochastic models were estimated using the corrected series. In such cases, the synthetic series metrics are compared to the stationary historical series.

In that regard, is worth noting that the differences between the original and corrected historical series metrics are relevant. For the South $ENAs$ and Foz do Areia streamflows (increasing trends), the larger discrepancies are in the mean and autocorrelation. Moreover, Foz do Areia also exhibits a significant difference in the maximum deficit. In turn, the Northeast $ENAs$ and Sobradinho streamflows (decreasing trends) produced divergences in the mean, standard deviation, and maximum deficits. The latter is notable mainly in the Northeast $ENAs$, representing a period with a significant energy deficit. These findings are important for the S-Y-R results to be discussed in the next section.

Table 6. P-values of the nonstationarity tests applied to the studied HPPs. Bold p-values indicate null hypothesis rejection at a 0.05 significance level. The signs in Mann-Kendall test results suggest increasing (+) or decreasing (–) trends.

HPP	Prewhitening	Mann-Kendall		Pettitt	
		p-value	Trend sign	p-value	Breakpoint (year)
Ilha Solteira	Yes	0.47	+	0.32	1971
Foz do Areia	Yes	**0.04**	+	0.06	1968
Sobradinho	Yes	**0.04**	–	**0.04**	1992
Tucuruí	Yes	0.73	–	0.72	1976

Table 7. ENAs synthetic series validation. Results for the South and Northeast subsystems are also shown for the original nonstationary series, for comparison.

Series	M (m³/s)	SD (m³/s)	CV	SK	min (m³/s)	max (m³/s)	AC1	LD (years)	MD (m³/s)
Southeast/Central-west									
Historical	41900	7183	0.17	0.44	28240	77520	0.38	9	54940
Synthetic	41820	6810	0.16	0.44	27710	61650	0.36	8.6	54710
South									
Historical (original)	9185	3249	0.35	0.82	3148	21720	0.24	7	17850
Historical (stationary)	10380	3356	0.32	0.52	4299	21720	0.11	8	16960
Synthetic	10360	3328	0.32	-0.01	2121	18590	0.10	6.3	20030
Northeast									
Historical (original)	7795	2578	0.33	0.72	2525	15130	0.53	11	36380
Historical (stationary)	5928	1666	0.28	0.57	2525	10140	0.41	8	16290
Synthetic	5910	1672	0.28	0.77	2889	11320	0.41	9.8	14370
North									
Historical	12360	2358	0.19	0.17	5838	18660	0.19	8	16520
Synthetic	12360	2329	0.19	-0.02	6888	17760	0.16	6	13630

Table 8. HPPs synthetic series validation. Results for Foz do Areia and Sobradinho are also shown for the original nonstationary series, for comparison.

Series	M (m³/s)	SD (m³/s)	CV	SK	min (m³/s)	max (m³/s)	AC1	LD (years)	MD (m³/s)
					Ilha Solteira				
Historical	5214	1184	0.23	0.98	2803	10680	0.42	9	9783
Synthetic	5202	1165	0.22	0.61	2949	8796	0.37	9.1	9523
					Foz do Areia				
Historical (original)	659	243	0.37	0.83	249	1528	0.24	5	513
Historical (stationary)	731	252	0.34	0.66	259	1528	0.14	5	1073
Synthetic	731	269	0.36	1.01	284	1680	0.11	7.6	1565
					Sobradinho				
Historical (original)	2531	840	0.33	0.73	796	4952	0.54	8	6127
Historical (stationary)	1942	555	0.28	0.58	796	3448	0.43	8	5466
Synthetic	1936	557	0.28	0.78	935	3744	0.43	10	4897
					Tucuruí				
Historical	10990	2957	0.27	0.74	6070	18880	0.34	7	24590
Synthetic	10980	2880	0.26	0.67	5858	19350	0.36	8.3	20670

S-Y-R relationships

EERs case

Considering that the *ENA* time series of the South and Northeast EERs presented evidence of nonstationarity in Mann-Kendall and Pettitt tests, we limited the application of the correction technique to these cases before obtaining the S-Y-R relationship. For the remainder two subsystems, we generated the S-Y-R curves using the original time series. (Figure 4).

For the Southeast/Central-West EER (Figure 4a), the S-Y-R relation is closer to the range between 60.5% and 77.8% (equivalent to a recurrence between 100 and 200 years) for most of the storage levels and regularization indexes. This implies that the reliability of this subsystem is practically constant regardless of its storage level. On the other hand, the South EER corrected S-Y-R curve (Figure 4b) crosses distinct reliability bands for different storage levels and regularization indexes. The largest variation is observed for the $\delta = 50\%$ to $\delta = 80\%$ interval, where the reliability increases from 36.4% to 81.8%, equivalently to a recurrence period between 50 and 250 years, respectively. Then, for $\delta > 80\%$ the reliability rises to values greater than 90%. For this EER, the effect of the nonstationarity can be observed when comparing the relations for the original and corrected series. In all storage levels, the stationary S-Y-R curve yielded higher regularization indexes, which can be explained by the identified increasing trend in the *ENA* time series.

For the Northeast EER (Figure 4c), the corrected S-Y-R relationship shows a constant reliability level (> 81.8%) for all regularization indexes. The nonstationary influence in this series is also evident since the original S-Y-R curve is out of the range of the reliability levels. However, this result should be analyzed carefully as it is not due to high levels of reliability (>90.5%). Rather, the synthetic series set was not able to mimic the most

severe drought period (e.g., critical period) of this EER's time series, as shown previously in Table 7. Recently, Detzel et al. (2019) suggested that the critical period of the HPPs operating in this subsystem changed from 1949-1956 to 2014-2017. Moreover, the severity of this recent drought was higher than in the former period. Hence, even though the stochastic model did reproduce the overall statistics of this time series, it failed to generate scenarios with droughts as severe as the recently observed. Therefore, we cannot assess the Northeast EER reliability levels for the original time series and suggest that it should be investigated in future studies.

Finally, for the North EER (Figure 4d) the S-Y-R relationship varies from 81.8-90.5% ($\delta = 60\%$), to 77.8-81.8% ($\delta > 80\%$), suggesting that higher regularization indexes imply lower reliability levels.

HPPs case

Besides the application of the nonstationarity correction technique (Foz do Areia and in Sobradinho), the results presented in this section are further detailed to add the S-Y-R relationship obtained for the opening date of each HPP. In these cases, the reliability levels were calculated using the synthetic scenarios generated with the model estimated with the historical dataset censured at the opening dates of the HPPs. In addition, a second set of S-Y-R curves is shown, in which we compare the curves calculated using the censured and complete time series. For this second analysis, the reliability levels were calculated using the updated time series (Figure 5).

The S-Y-R for Ilha Solteira (Figure 5a) shows that the relative regularization capacity slightly decreased when comparing both periods. Given the useful storage capacity (Table 1), this reduction is 6.2% (from $\delta = 65\%$ to $\delta = 61\%$). Despite this relative loss, the original curve (1931-1973) has not changed from its previous
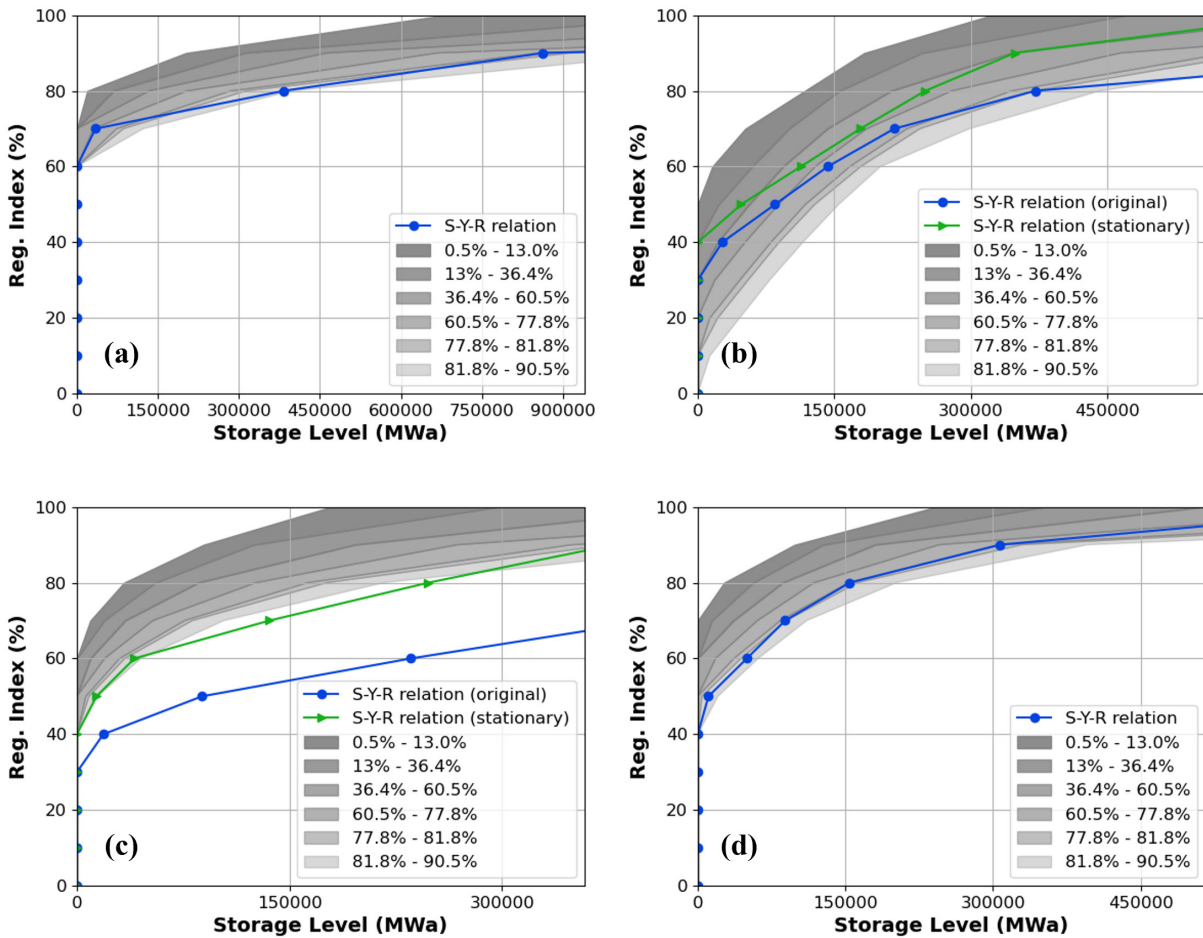
Figure 4. S-Y-R relationships for each EER: (a) Southeast/Central-West, (b) South, (c) Northeast, and (d) North. The blue and green curves were obtained with the historical series. The shades indicate the different reliability bands for the S-Y-R curves.

reliability band (36.4-60.5% range). However, when considering the updated S-Y-R relationship, we can conclude that there was an increase in the reliability level when compared to the original period (from 36.4-60.5% to 77.8-90.5%).

In Foz do Areia (Figure 5b) the relative regularization capacity loss is more evident. This case can be understood as a direct outcome of the increase in the Iguazu River streamflow time series. As mentioned earlier, the relation between the long-term mean and regularization index is inverse, which explains the result. We estimate the relative regularization capacity reduction to be 7.4% (from $\delta = 61\%$ to $\delta = 56\%$), but there was no change in the reliability bands of the original curve (1931-1981) over time. Nonetheless, it could be a direct consequence of the nonstationary correction previously made in the HPP series. In fact, the increase in the average streamflow should allow Foz do Areia to meet its original yield more securely. On the other hand, if it operates with the same regularization index which it was designed for, the storage capacity should be higher, as well as the operational risk.

Sobradinho (Figure 5c) presents two very different results between the S-Y-R relationships. Considering its useful storage capacity, the plot on the left panel reveals that the reliability level was in the 36.4-60.5% band when the reservoir was designed. In turn, the plot on the right panel suggests that this reliability

decreased to the 13.0-36.4% band for the updated S-Y-R curves. Moreover, the results show a 38.5% loss in the relative regularization capacity (from $\delta = 78\%$ to $\delta = 48\%$). However, these findings should also be analyzed with caution, as Sobradinho is in the Northeast subsystem and, hence, suffered from the same severe drought period in the 2010s mentioned earlier. The consequences of this period are seen when comparing both plots since only the S-Y-R relationships (red curve and reliability bands) on the right panel were obtained with the data that contained the 2010s drought. Therefore, in the same fashion that the Northeast ENAs S-Y-R results, we argue that the updated reliability level for Sobradinho cannot be assessed here because of the limitation of the stochastic model in representing such a severe drought period (see Table 8).

Finally, Tucuruí's (Figure 5d) S-Y-R curves are similar between periods, as expected for having a stationary streamflow time series. The loss in the relative regularization capacity is 1.9% (from $\delta = 52.5\%$ to $\delta = 51.3\%$), which can be considered a variation derived from different lengths of the time series. Nonetheless, when analyzing the reliability bands, the curves have not changed, which indicates no increase in the operational risk. Also, the updated S-Y-R curve practically crosses the boundary between the bands, which may be an effect of the sample size variations.
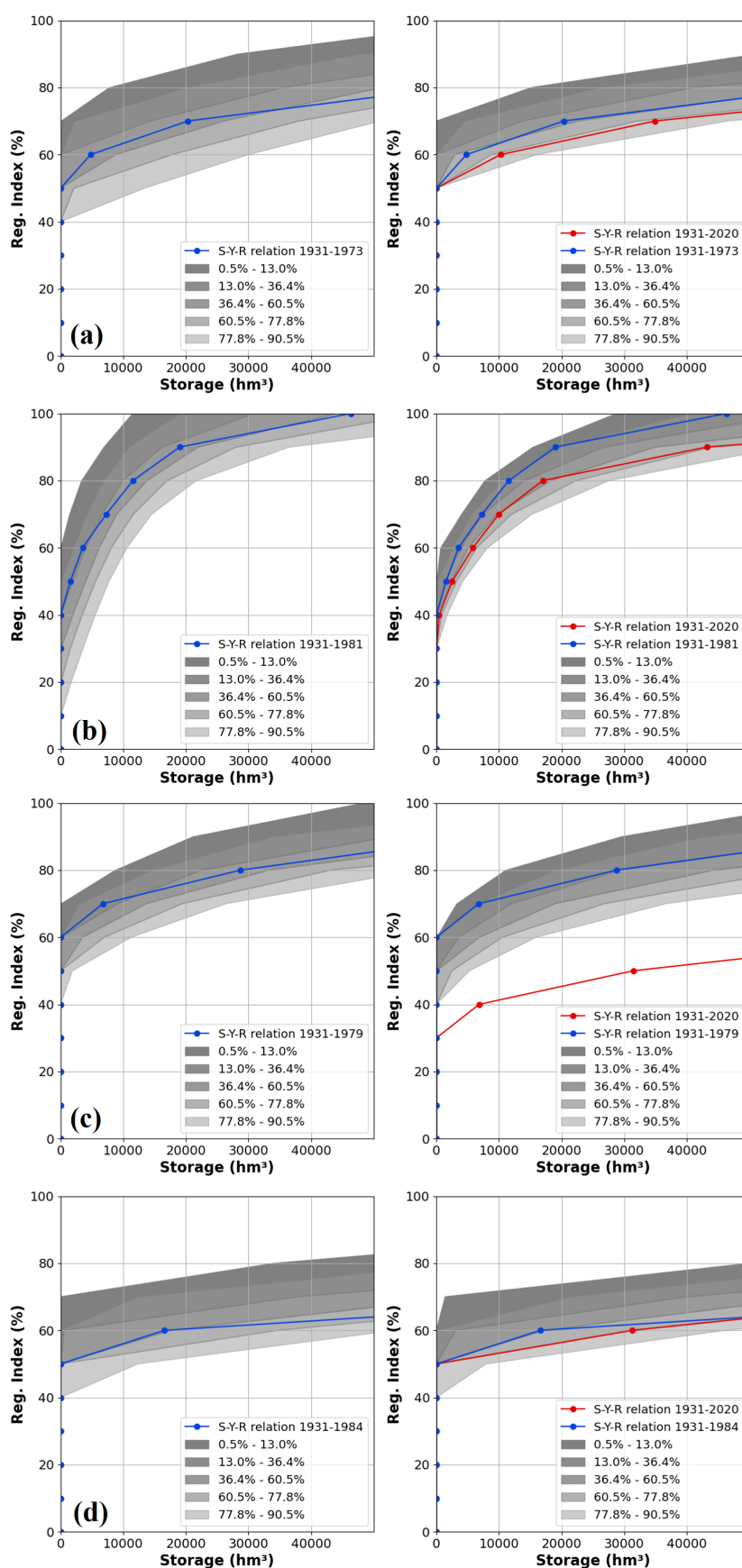
Figure 5. S-Y-R relationships for each HPP: (a) Ilha Solteira, (b) Foz do Areia, (c) Sobradinho, and (d) Tucuruí. On the left panel, the reliability levels were obtained with the model estimated with the historical dataset censured at the opening dates of the HPPs. On the right panel, they were calculated using all the available data.

CONCLUSION

The fact that the regularization index is inversely related to the long-term mean of the streamflow time series suggests that an increasing trend in such a mean would cause a loss in the S-Y-R relationships. In this paper, we show that this was the case for Foz do Areia HPP, as the regularization index of its reservoir dropped 7.4%. It should be noted, however, that this loss is relative to the value of the updated long-term mean. Since this mean is higher than the time when the HPP was constructed, the reservoir can meet the original yield (in m³/s) more securely. On the other hand, should it be operated with the same regularization index that it was designed, the storage capacity should be higher, as well as the operational risk. In this particular case, the loss in the regularization capacity was not a strictly negative factor, since, as mentioned before, this loss was only relative to the HPP's average streamflow. Furthermore, Foz do Areia HPP streamflow series presented a nonstationarity behavior, with an upward trend over time.

Sobradinho HPP streamflow series also presented a non-stationarity behavior, however, unlike Foz do Areia series, the trend identified was downward. A non-expected result was that, for both series, despite the nature of their trends, there was a relative loss in the regularization capacity over time. When analyzing Sobradinho's updated regularization curve, it is possible to conclude that the reservoir had an actual loss in its regularization capacity. Since the HPPs' useful storage is constant, the regularization index depends exclusively on the reservoir demand. Sobradinho cannot safely meet its original demand (e.g. original δ) without increasing the operational risk, once the current streamflow series mean is inferior when compared to the original one.

For all other cases, the study revealed that changes in the regularization capacity and reliability bands are expected to occur even with reservoirs with stationary inflows, however milder than the ones with non-stationarity behavior, as observed in Sobradinho. In that sense, the results of trends and/or breakpoints in streamflow time series should not be used as a definitive criterion for developing analyzes regarding regularization capacity. Therefore, we recommend that the operational rules of reservoirs should be continuously revised together with the increase in the time series' lengths.

ACKNOWLEDGEMENTS

REFERENCES

Abou Rafee, S. A., Uvo, C. B., Martins, J. A., Machado, C. B., & Freitas, E. D. (2022). Land Use and Cover Changes versus climate shift: who is the main player in river discharge? A case study in the Upper Paraná River Basin. *Journal of Environmental Management*, *309*, 114651. PMid:35151138. http://dx.doi.org/10.1016/j.jenvman.2022.114651.

Akaike, H. (1974). A new look at the statistical model identification. *IEEE Transactions on Automatic Control*, *19*(6), 716-723. http://dx.doi.org/10.1109/TAC.1974.1100705.

Aljoda, A., & Jain, S. (2021). Uncertainties and risks in reservoir operations under changing hydroclimatic conditions. *Journal of Water and Climate Change*, *12*(5), 1708-1723. http://dx.doi.org/10.2166/wcc.2020.133.

Agência Nacional de Energia Elétrica – ANEEL. (2022). *Sistema de Informações de Geração da ANEEL – SIGA*. Retrieved in 2022, April 2, from https://bit.ly/2IGf4Q0

Box, G. E. P., Jenkins, G. M., & Reinsel, G. C. (2008). *Time series analysis forecasting and control* (4th ed.). New Jersey: John Wiley & Sons.

Braga, R. S., Rocha, V. F., & Gontijo, E. A. (2009). Revisão das séries de vazões naturais nas principais bacias hidrográficas do Sistema Interligado Nacional. In *Anais do XVIII Simpósio Brasileiro de Recursos Hídricos*. Campo Grande: ABRHidro.

Briscoe, J. (2011). Making reform happen in water policy: reflections from a practitioner. In *OECD Global Forum on Environment: Making Water Reform Happen*. Paris.

Brown, A. E., Zhang, L., McMahon, T. A., Western, A. W., & Vertessy, R. A. (2005). A review of paired catchment studies for determining changes in water yield resulting from alterations in vegetation. *Journal of Hydrology*, *310*(1-4), 28-61. http://dx.doi.org/10.1016/j.jhydrol.2004.12.010.

Carvalho, A. R. (2015). *Reservatórios de regularização de usinas hidrelétricas: contribuição para uma matriz elétrica mais limpa* (Tese de doutorado). COPPE, Universidade Federal do Rio de Janeiro, Rio de Janeiro.

Chagas, V. B. P., & Chaffe, P. L. B. (2018). The role of land cover in the propagation of rainfall into streamflow trends. *Water Resources Research*, *54*(9), 5986-6004. http://dx.doi.org/10.1029/2018WR022947.

Detzel, D. H. M., Martini Filho, L. R., Rangel, L. M. A., Bessa, M. R. D., & de Geus, K. (2019). Acerca do período crítico das usinas hidrelétricas brasileiras. In *Anais do XXIII Simpósio Brasileiro de Recursos Hídricos*. Foz do Iguaçu: ABRHidro.

Detzel, D., Bessa, M., Vallejos, C., Santos, A., Thomsen, L., Mine, M., Bloot, M., & Estrocio, J. (2011). Estacionariedade das afluências às usinas hidrelétricas brasileiras. *RBRH*, *16*(3), 95-111. http://dx.doi.org/10.21168/rbrh.v16n3.p95-111.

Dore, M. H. I. (2005). Climate change and changes in global precipitation patterns: what do we know? *Environment International*, *31*(8), 1167-1181. PMid:15922449. http://dx.doi.org/10.1016/j.envint.2005.03.004.

Ehsani, N., Vörösmarty, C. J., Fekete, B. M., & Stakhiv, E. Z. (2017). Reservoir operations under climate change: storage capacity options to mitigate risk. *Journal of Hydrology*, *555*, 435-446. http://dx.doi.org/10.1016/j.jhydrol.2017.09.008.

Fleming, S. W., & Weber, F. A. (2012). Detection of long-term change in hydroelectric reservoir inflows: bridging theory and practise. *Journal of Hydrology*, *470-471*, 36-54. http://dx.doi.org/10.1016/j.jhydrol.2012.08.008.

Freitas, G. N. (2020). São Paulo drought: trends in streamflow and their relationship to climate and human-induced change in Cantareira watershed, Southeast Brazil. *Nordic Hydrology*, *51*(4), 750-767. http://dx.doi.org/10.2166/nh.2020.161.

Gleick, P. H. (1989). Climate change, hydrology, and water resources. *Reviews of Geophysics*, *27*(3), 329-344. http://dx.doi.org/10.1029/RG027i003p00329.

Gudmundsson, L., Leonard, M., Do, H. X., Westra, S., & Seneviratne, S. I. (2019). Observed trends in global indicators of mean and extreme streamflow. *Geophysical Research Letters*, *46*(2), 756-766. http://dx.doi.org/10.1029/2018GL079725.

Guo, Y., Fang, G., Xu, Y. P., Tian, X., & Xie, J. (2020). Identifying how future climate and land use/cover changes impact streamflow in Xinanjiang basin, east China. *The Science of the Total Environment*, *710*, 136275.

Heerspink, B. P., Kendall, A. D., Coe, M. T., & Hyndman, D. W. (2020). Trends in streamflow, evapotranspiration, and groundwater storage across the Amazon Basin linked to changing precipitation and land cover. *Journal of Hydrology. Regional Studies*, *32*, 100755. http://dx.doi.org/10.1016/j.ejrh.2020.100755.

Kendall, M. G. (1975). *Rank correlation methods*. London: Griffin.

Kuria, F., & Vogel, R. (2015). Uncertainty analysis for water supply reservoir yields. *Journal of Hydrology*, *529*, 257-264. http://dx.doi.org/10.1016/j.jhydrol.2015.07.025.

Larroyd, P. V., de Matos, V. L., & Finardi, E. C. (2017). Assessment of risk-averse policies for the long-term hydrothermal scheduling problem. *Energy Systems*, *8*(1), 103-125. http://dx.doi.org/10.1007/s12667-016-0191-y.

Lee, E., Livino, A., Han, S. C., Zhang, K., Briscoe, J., Kelman, J., & Moorcroft, P. (2018). Land cover change explains the increasing discharge of the Paraná River. *Regional Environmental Change*, *18*(6), 1871-1881. PMid:30996672. http://dx.doi.org/10.1007/s10113-018-1321-y.

Levy, M. C., Lopes, A. V., Cohn, A., Larsen, L. G., & Thompson, S. E. (2018). Land use change increases streamflow across the arc of deforestation in Brazil. *Geophysical Research Letters*, *45*(8), 3520-3530. http://dx.doi.org/10.1002/2017GL076526.

Loucks, D. P., & van Beek, E. (2005). *Water resources systems planning and management*. Retrieved in 2022, April 2, from https://www.springer.com/gp/book/9783319442327.

Mann, H. B. (1945). Non-parametric tests against trend. *Econometrica*, *13*(3), 245-259. http://dx.doi.org/10.2307/1907187.

McMahon, T. A., Vogel, R. M., Pegram, G. S., Peel, M. C., & Etkin, D. (2007). Global streamflows – Part 2: reservoir storage–yield performance. *Journal of Hydrology*, *347*(3-4), 3-4, 260-271. http://dx.doi.org/10.1016/j.jhydrol.2007.09.021.

Milly, P. C. D., Betancourt, J., Falkenmark, M., Hirsch, R. M., Kundzewicz, Z. W., Lettenmaier, D. P., Stouffer, R. J., Dettinger, M. D., & Krysanova, V. (2015). On critiques of "stationarity is dead: whither water management?". *Water Resources Research*, *51*(9), 7785-7789. http://dx.doi.org/10.1002/2015WR017408.

Mo, G., Zhang, Y., Huang, Y., Mo, C., & Yang, Q. (2020). Evaluation and hydrological impact of land-use changes in the Longtan basin. *Journal of Earth System Science*, *129*(1), 190. http://dx.doi.org/10.1007/s12040-020-01458-1.

Neira, K. L. (2005). *Curvas de regularização para reservatórios parcialmente cheios e confiabilidade constante* (Dissertação de mestrado). Programa de Pós-graduação em Engenharia de Recursos Hídricos e Ambiental, Universidade Federal do Paraná, Curitiba.

Operador Nacional do Sistema Elétrico – ONS. (2020). Retrieved in 2020, December 16, from http://www.ons.org.br/paginas/sobre-o-sin/mapas

Jong, P., Tanajura, C. A. S., Sánchez, A. S., Dargaville, R., Kiperstok, A., & Torres, E. A. (2018). Hydroelectric production from Brazil's São Francisco River could cease due to climate change and inter-annual variability. *The Science of the Total Environment*, *634*, 1540-1553. PMid:29710652. http://dx.doi.org/10.1016/j.scitotenv.2018.03.256.

Pettitt, A. N. (1979). A non-parametric approach to the change-point problem. *Applied Statistics*, *28*(2), 126-135. http://dx.doi.org/10.2307/2346729.

Salas, J. D., Delleur, J. W., Yevjevich, V., & Lane, W. L. (1985). *Applied modeling of hydrologic time series* (2nd ed.). Chelsea: Water Resources Publications.

Schwartz, G. (1978). Estimating the dimension of a model. *Annals of Mathematical Statistics*, *6*(2), 461-464.

Silva, W. L., Xavier, L. N. R., Maceira, M. E. P., & Rotunno, O. C. (2019). Climatological and hydrological patterns and verified trends in precipitation and streamflow in the basins of Brazilian hydroelectric plants. *Theoretical and Applied Climatology*, *137*(1-2), 353-371. http://dx.doi.org/10.1007/s00704-018-2600-8.

Silva, A. T., & Portela, M. M. (2013). Stochastic assessment of reservoir storage-yield relationships in Portugal. *Journal of Hydrologic*

Engineering, *18*(5), 5. http://dx.doi.org/10.1061/(ASCE)HE.1943-5584.0000650.

Srivastava, D. K., & Awchi, T. A. (2009). Storage-yield evaluation and operation of Mula Reservoir, India. *Journal of Water Resources Planning and Management*, *135*(6), 6. http://dx.doi.org/10.1061/(ASCE)0733-9496(2009)135:6(414).

Vogel, R. M., Sieber, J., Archfield, S. A., Smith, M. P., Apse, C. D., & Huber-Lee, A. (2007). Relations among storage, yield, and instream flow. *Water Resources Research*, *43*(5), W05403. http://dx.doi.org/10.1029/2006WR005226.

Vogel, R. M., Lane, M., Ravindiran, R. S., & Kirshen, P. (1999). Storage reservoir behavior in the United States. *Journal of Water Resources Planning and Management*, *125*(5), 245-254. http://dx.doi.org/10.1061/(ASCE)0733-9496(1999)125:5(245).

Vogel, R. M., Bell, C. J., & Fennessey, N. M. (1997). Climate, streamflow and water supply in Northeastern United States. *Journal of Hydrology*, *198*(1-4), 42-68. http://dx.doi.org/10.1016/S0022-1694(96)03327-6.

Vogel, R. M., & McMahon, T. A. (1996). Approximate reliability and resilience indices of over-year reservoirs fed by AR(1) gamma and normal flows. *Hydrological Sciences Journal*, *41*(1), 75-96. http://dx.doi.org/10.1080/02626669609491480.

Vogel, R. M., & Bolognese, R. A. (1995). Storage-reliability-resilience-yield relations for overyear water supply systems. *Water Resources Research*, *31*(3), 645-654. http://dx.doi.org/10.1029/94WR02972.

Vogel, R. M., Fennessey, N. M., & Bolognese, R. A. (1995). Storage-reliability-resilience-yield relations for Northeastern United States. *Journal of Water Resources Planning and Management*, *121*(5), 365-374. http://dx.doi.org/10.1061/(ASCE)0733-9496(1995)121:5(365).

Vogel, R. M., & Stedinger, J. R. (1988). The value of stochastic streamflow models in overyear reservoir design applications. *Water Resources Research*, *24*(9), 1483-1490. http://dx.doi.org/10.1029/WR024i009p01483.

Vogel, R. M., & Stedinger, J. R. (1987). Generalized reservoir storage-reliability-yield relationships. *Journal of Hydrology*, *89*(3–4), 303-327. http://dx.doi.org/10.1016/0022-1694(87)90184-3.

Wang, W., Shao, Q., Yang, T., Peng, S., Xing, W., Sun, F., & Luo, Y. (2013). Quantitative assessment of the impact of climate variability and human activities on runoff changes: a case study in four catchments of the Haihe River basin, China. *Hydrological Processes*, *27*(8), 1158-1174. http://dx.doi.org/10.1002/hyp.9299.

Yue, S., Pilon, P., Phinney, B., & Cavadias, G. (2002). The influence of autocorrelation on the ability to detect trend in hydrological series. *Hydrological Processes*, *16*(9), 1807-1829. http://dx.doi.org/10.1002/hyp.1095.

Authors contributions

Henrique Degraf: Responsible by the streamflow data download from ONS portal, programming the codes used for the article, image formatting, text review.

Daniel Henrique Marco Detzel: Responsible by the streamflow data download from ONS portal, for the article, text review.

Editor-in-Chief: Adilson Pinheiro

Associated Editor: Carlos Henrique Ribeiro Lima